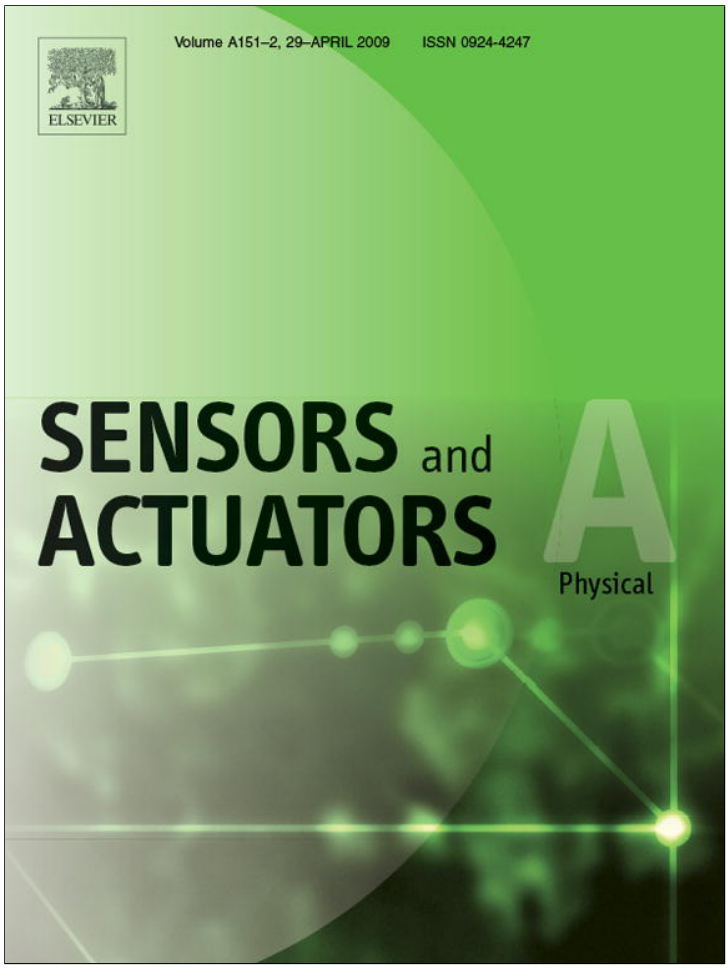

Sensors and Actuators A 151 (2009) 213–219

Contents lists available at ScienceDirect

Sensors and Actuators A: Physical

journal homepage: www.elsevier.com/locate/sna

Development of temperature feedback control system for piezo-actuated display package

Jae Choon Kim[a], Jin Taek Chung[a,*], Dong Jin Lee[b], Yong-Kook Kim[b], Jin Woo Kim[a], SungWoo Hwang[b], Byeong-Kwon Ju[b], Sang Kyeong Yun[c], Heung-Woo Park[c]

[a] Department of Mechanical Engineering, Korea University, Republic of Korea
[b] Department of Electronic and Computer Engineering, Korea University, Republic of Korea
[c] SOM R&D and Biz Group, OS Division, Samsung Electro-Mechanics Co., Republic of Korea

ARTICLE INFO

Article history:
Received 1 November 2008
Received in revised form 9 February 2009
Accepted 11 February 2009
Available online 28 February 2009

Keywords:
Microheater
Thermal analysis
Temperature control
Deformable mirror
Display package

ABSTRACT

This paper describes a temperature management system for a deformable mirrors of piezo-actuated display package (PADP). This package which is integrated in microbeam projectors is used in portable devices such as cellphones, laptops, and personal digital assistants (PDAs), to name a few. Ambient temperature change is a critical factor affecting the performance of PADP. To reduce this effect of ambient temperature change, a temperature control system using a microheater and a temperature feedback circuit is developed. A computational model of the transient thermal analysis for the feedback control system is also developed. The obtained theoretical results are in a good agreement with the experimental measurements. Under this controlled system, the magnitude of the temperature fluctuation is reduced by ±0.5 °C. In order to enhance the performance of the developed system, various values of the temperature sensor resistance are used, leading to a reduction of about 10% of the temperature fluctuation.

1. Introduction

Recently, projection displays embedded in portable devices such as cellular phones, laptops, and personal digital assistants (PDAs) [1] have been widely studied. The temperature-related problems are encountered as the projection display becomes smaller and lighter due to higher resolution. The piezoelectric actuator is temperature dependent [2,3]. Hence, the display packages driven by piezoelectric actuator are sensitive to the ambient temperature. For instance, during winter, there is a decrease in the operating temperature of a display package. This results in a drastic change in the position of the internal deformable mirrors. The large deformation of the mirrors emits distorted beams producing poor images on the screen. The effect of surrounding temperature on the diffraction efficiency of a deformable mirror was shown by Bouyge et al. [4]. However, until now there is no solution for this problem.

The design of cooling systems, and the thermal design of projectors and their display packages, has been widely studied. Nevertheless, remedies to solve temperature induced malfunctions in a display package are insufficient to the date. In the past, microheaters for temperature control were used for common devices such as gas sensors, flow sensors, and temperature sensors [5,6]. Gong et al. [7] studied the temperature control methods and designed a control circuit sensor. However, there were certain limitations in the controlled temperature range, the supplied temperature and the current. Thus it was difficult to apply the circuit directly to the display package. Hence, these studies are not applicable to projection displays embedded in mobile devices. We have been, so far, unsuccessful in finding references showing a clear solution to the malfunctioning of a projection display package caused by the surrounding temperature.

In the present study, microheaters and their feedback control circuits have been fabricated on a projection display package embedded in a portable device. The microheaters and temperature sensors are designed using numerical and experimental methods. A semiconductor manufacturing process is used for fabrication. The effects of the operation of the microheaters are analyzed, and the time periods for switching the microheater on and off are considered in the numerical analysis. It is concluded that the time step for the microheater operation should be at least 8.12 μs.

Ambient temperature is the parameter used to evaluate the performance of the microheater and control circuit. A temperature control device made of a thermoelectric cooler and a heat exchanger is developed to change the ambient temperature. A platinum temperature sensor is used in this study. Platinum temperature sensor can measure the temperature precisely and this resistance of platinum temperature sensor can be converted to the temperature change of the module. The temperature change, thus obtained, can

* Corresponding author. Tel.: +82 2 3290 3758; fax: +82 2 928 9766.
E-mail address: jchung@korea.ac.kr (J.T. Chung).

0924-4247/$ – see front matter © 2009 Elsevier B.V. All rights reserved.
doi:10.1016/j.sna.2009.02.019

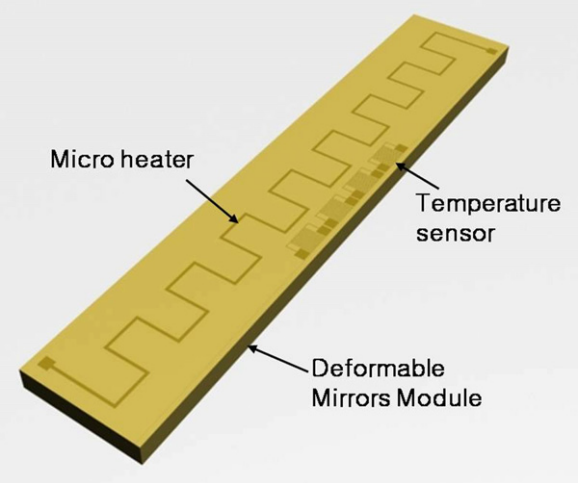

Fig. 1. Schematic of microheater.

be used for feedback control. As a result, the operating temperature automatically adapted to the surrounding temperature changes, and a predefined operating temperature is maintained. The thermal characteristic of the display module mounted on the projection display package is obtained. The magnitude of the temperature fluctuation of 1 °C is achieved.

The effects of the resistance value of the temperature sensor on temperature control are investigated using four different magnitudes of resistance. The magnitude of the controlled temperature fluctuation and the time period for switching the microheater on and off are determined. As a result, the relationship between the sensor's resistance value and performance is obtained. It is expected that the present method would improve the performance of piezo-actuated display packages (PADP) and be useful in the implementation of piezoelectric actuators into commercial electronic devices.

2. Design and fabrication

2.1. Design and fabrication of the microheater

2.1.1. Microheater geometry

Fig. 1 shows the design of the microheater. The general requirements for a thin film microheater are low power consumption, fast response, good heat uniformity, good mechanical stability, and good fabrication yield [8]. Hence, gold (Au) is selected as the microheater material, and chromium (Cr) is used in the adhesion layer between the Au and the silicon module. High resistivity is useful for a temperature sensor that requires high resistance. Moreover, a temperature sensor of high resistance is more sensitive to temperature change than a temperature sensor of low resistance. Platinum (Pt) is selected as the temperature sensor due to its good thermal coefficient and high resistivity. The Pt temperature sensor consists of four resistors (see Fig. 1). Four resistance values are used to investigate the effect of temperature sensor resistance on magnitude of temperature fluctuation. The microheater and temperature sensors are attached to the rear of the deformable mirrors. Note that the thermal resistance between microheater and deformable mirrors is negligible.

2.1.2. Fabrication of the microheater

The process flow of simplified microfabrication for the microheater and temperature sensor is shown in Fig. 2. A 0.525 mm silicon wafer is used as the substrate for the microheater and sensor. The fabrication of the microheater is performed using microfabrication technology as follows:

1. The substrate with 300 nm SiO_2 is laminated with Plasma-enhanced chemical vapor deposition (PECVD) for the dielectric at the rear of the deformable mirrors.
2. A 30 nm Cr and 300 nm Au are deposited on the silicon substrate by e-beam evaporation. The Cr layer acts as both the resistor and adhesion layer between Au and the substrate.
3. A positive photoresist is spin-coated onto the Au layer and patterned using photolithography through mask #1.
4. Dry etching is conducted to remove metal that is not used in making the heater.
5. A negative photoresist is spin-coated to fabricate the temperature sensor.
6. The patterning was carried out using mask #2.
7. 30 nm titanium (Ti) and 150 nm Pt are deposited on the substrate by e-beam evaporation. Note that the Ti layer acts as both the resistor and adhesion layer between Pt and the substrate.
8. Finally, the heater and sensor are formed by lift-off.

A detailed microscopic view of a fabricated device is shown in Fig. 3.

2.2. Temperature feedback control circuit

Fig. 4 shows the temperature feedback circuit. The feedback circuit is driven by voltage. The Pt temperature sensor can be considered to be a resistor. The resistance change of the Pt temperature sensor due to heat is transformed into a change in voltage at P, V_p. V_p can be calculated for Eq. (1)

$$V_p = \frac{R_{sensor}}{(R_A + R_{sensor})} \times V_s \quad (1)$$

where R_{sensor} is the resistance of Pt temperature sensor.

The comparator compares the V_s to match the operating temperature with V_p. For instance, if V_p is lower than working V_s, the comparator generates a 'high' signal and the MOSFET is switched on. Thus, the current flows across the heater and heater is switched on. On the contrary, if V_p is higher than working V_s, the comparator does not generate a signal, and MOSFET is switched off. The temperature feedback control system, thus, automatically maintain the operating temperature.

2.3. Pt temperature coefficient of resistance

Pt is selected as the temperature sensor material because of its linear thermal coefficient and stability at elevated temperature. However, the resistance of Pt film depends on the fabrication and the thickness [9]. The Pt temperature sensor's thermal coefficient is calibrated to obtain proper resistance behavior. The resistance can be written as a function of temperature as follows:

$$R = R_0[1 + \alpha(T - T_0)] \quad (2)$$

where T is the change in temperature, T_o is the initial temperature, R_o is the resistance at the reference temperature and α is the temperature coefficient of the resistance (TCR). For thin-film Pt TCR is found to be $3.927 \times 10^{-3}\,K^{-1}$ [10].

The measured sensor temperatures are used to calibrate the temperature coefficient of the Pt temperature sensor when the input power is controlled. A method to calibrate the Pt temperature sensor by controlling input power was introduced by Gong [7]. Another approach, different from controlling of input power, is used in this work to calibrate the Pt temperature sensor. A device composed of the thermoelectric coolers (TEC) and the heat exchanger is used to control the ambient temperature. The temperature of the

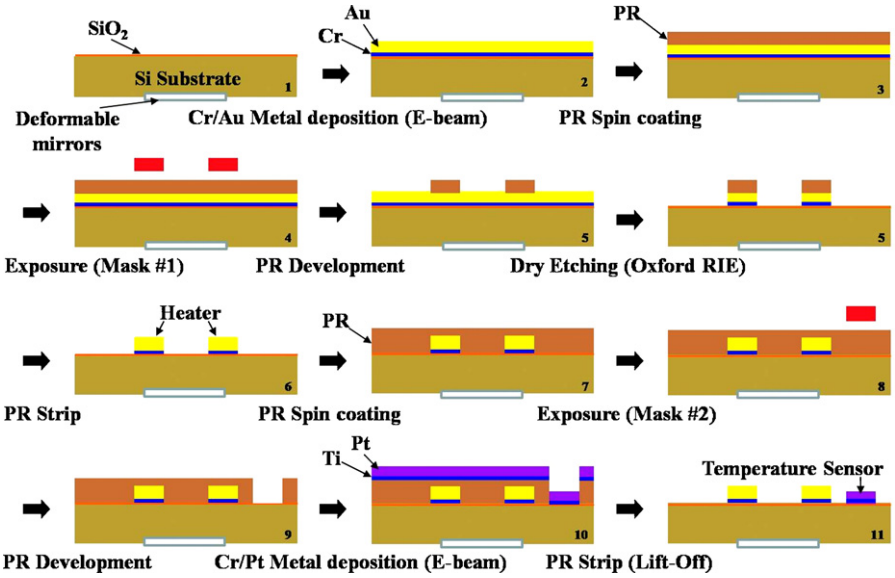

Fig. 2. Schematic of micro-fabrication process flow.

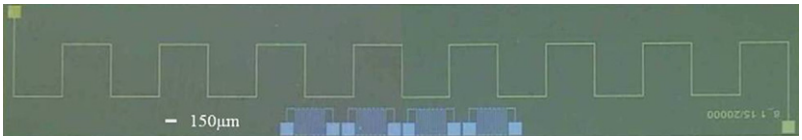

Fig. 3. Details of microheater and temperature sensors.

module is measured using thermocouples and an infrared camera. The thermo-couple is placed at the module, and the infrared camera is set up above the module. The resistance values of the Pt sensor are measured for ambient temperatures between 0 °C and 60 °C, in increments of 0.1 °C. Fig. 5 shows Pt temperature sensor resistance versus temperature change. Here, TS1 (0.982 k Ω) is a separate resistor whereas TS2 (2.134 k Ω) is the connection between two separate resistors with wire bonding. TS3 (3.361 k Ω) and TS4 (4.374 k Ω) are also obtained using the connection of four resistors, as shown in Fig. 1. The deviation in the rate of increase in resistance is less than 2%. From these processes, the TCR of the Pt temperature sensor is determined to be 2.3×10^{-3} K^{-1}. The measured hysteresis values of these sensors, TS1, TS2, TS3, and TS4, are 0.15%, 0.29%, 0.21%, and 0.25% respectively. These values are negligible and do not affect the temperature control.

3. Numerical method and experimental method

3.1. Numerical method

3.1.1. Three-dimensional finite volume method

The simulations are performed on Flotherm, a commercial computational fluid dynamics (CFD) tool based on the finite volume method. Flotherm solves airflow and heat transfer problems in and around electronic equipments. The tool solves fully conjugated heat transfer problems (all three modes – conduction, convection, and

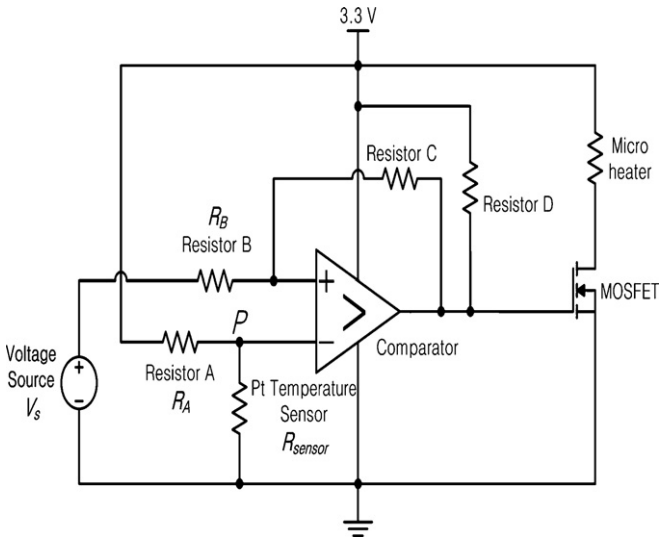

Fig. 4. Feedback control circuit.

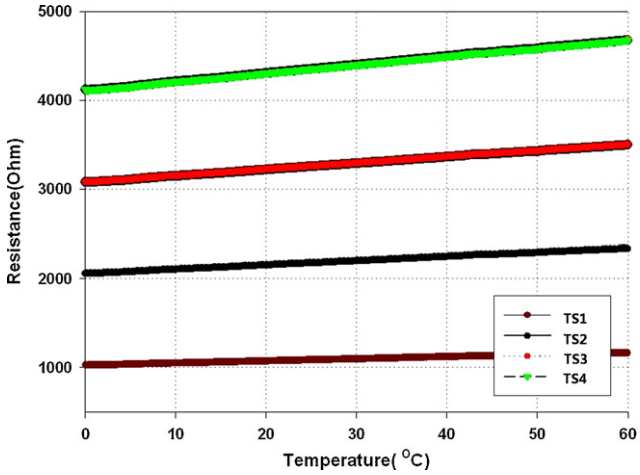

Fig. 5. Ambient temperature effect on the resistance of Pt sensor.

Table 1
Average temperature of module along number of mesh.

Number of mesh	50,000	100,000	150,000	200,000	250,000
Average temperature of module (°C)	76.04	75.07	62.77	62.78	62.74

radiation – are considered). The air flow and heat transfer processes are governed by the conservation equations of mass, momentum and energy and are detailed below.

Mass conservation

$$\frac{\partial \rho}{\partial t} + \nabla \cdot (\rho \vec{u}) = 0 \tag{3}$$

Momentum conservation

$$\frac{\partial (\rho \vec{u})}{\partial t} + \nabla \cdot (\rho \vec{u} \vec{u}) = \rho g_i - \nabla P + \mu \nabla^2 \vec{u} \tag{4}$$

Energy conservation

$$\frac{\partial (\rho h)}{\partial t} + \nabla (\rho \vec{u} h) = \kappa \nabla^2 T + S_h \tag{5}$$

The temperature of ambient air is fixed at 20 °C and a natural convection environment is applied to the simulation. All material properties are taken from the material database [11]. The total number of grid points is optimized using the localized and nesting meshes. The average temperature of the model obtained by considering different number of points is shown in Table 1. It can be seen that the solution converges after around 150,000 grid points. The computational results are obtained by considering 160,000 grid points.

3.1.2. Temperature feedback control

Feedback control is selected as the control algorithm for the microheater. A transient numerical simulation is conducted to obtain the thermal characteristics of the display module with feedback control. Feedback control for temperature maintenance is achieved by switching on/off the microheater when overcooled/overheated. The maximum response time of the comparator is 8 μs, and the maximum time for which the MOSFET is on is 120 ns [12,13]. This implies that the circuit should be switched on for at least 8.12 μs. Thus, the time step of the microheater operation was obtained

3.2. Experimental method

The microheater is installed on a deformable mirror module as shown in Fig. 6. The temperature is measured by an infrared camera and thermocouple. The size of the module restricts the use of thermocouple to measure the temperature on the surface of the deformable mirror. The heat spread through the thermocouple wire could affect the results if it detects the temperature of the small device. Hence, the two temperature detectors were used for precise temperature measurement. The specification of the infrared camera is given in Table 2. The temperature of the display module was measured with the setup depicted in Fig. 7. The various components of the device have different emissivity values, see Fig. 6. A direct measurement of the temperature from raw surfaces could result in unrealistic temperature values. Hence, the board was coated with black paint with known emissivity (e = 0.97). Thus, all components had the same emissivity. A temperature distribution was then obtained directly from the IR picture.

Table 2
Specification of infrared camera.

Pixel number	320 × 240 pixels
1 Pixel area	100 μm²
Thermal sensitivity	0.08 °C
Spatial resolution	1.3 mrad
Sample rate	60 Hz

4. Results and discussion

4.1. Temperature–power relationship

The temperature of the deformable mirror module with respect to the power of the microheater is investigated. This is to achieve the optimum power of the microheater required to maintain the operating temperature. The thermal resistance of the module is 0.35 K/W and it is small enough to be neglected. Most portable projector manufacturers ignore the minimum ambient temperature and assume a maximum ambient temperature between 35 °C and 40 °C [14]. In this study, the ambient temperature is varied from 0 °C to 40 °C. The operating temperature is taken to be 40 °C and a microheater assists in maintaining this operating temperature. Further experimental analysis shows that the power of the microheater should be set to 0.3 W.

4.2. Thermal uniformity

The thermal uniformity of the deformable mirrors is of utmost importance. This is because enormous numbers of deformable mirrors are arranged laterally. The lateral arrangement of the mirrors is shown in Fig. 2. The thermal uniformity of the module is ensured by conducting various transient numerical and experimental analyses. Fig. 8(a) shows the simulated temperature distribution of the cross section of the module at the position of the deformable mirrors. The maximum temperature is about 40 °C with the ambient of 20 °C. The difference between maximum and minimum temperatures is less than 0.1 °C at the surface of the deformable mirror module. Fig. 8(b) shows the thermal image at the module surface. The difference between maximum and minimum temperatures is less than 0.3 °C at the surface of the deformable mirror module. The temperature distributions from the numerical analysis and the experiment study are in good agreement.

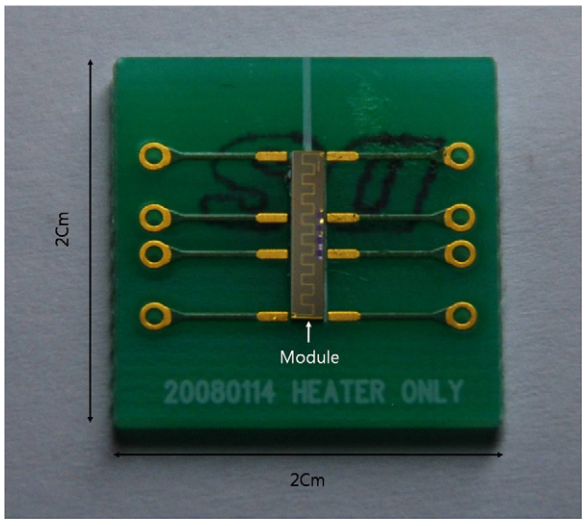

Fig. 6. Top view photograph of the device.

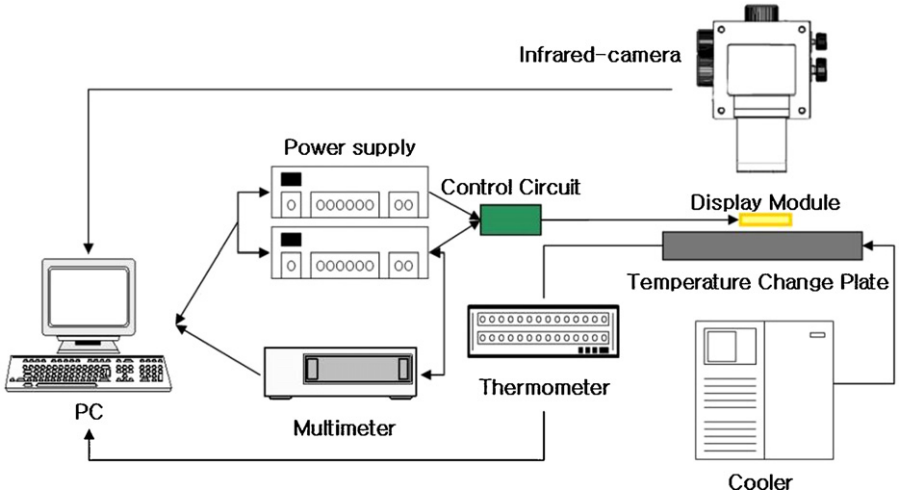

Fig. 7. Experimental setup for performance test of temperature control system.

4.3. Temperature feedback control

The thermal characteristics of the deformable mirror module with feedback control are analyzed using numerical and experimental methods. Fig. 9 shows the temperature of the deformable mirror obtained from numerical simulation and experimental observations when temperature feedback is applied. The numerical results show a gradual increase in the temperature from 20 °C to 40 °C 2.2 s. After this time, the temperature fluctuates in the range of about ±0.5 °C. In the experimental observation the fluctuation characteristic is also achieved after 40 °C but approximately after 2.8 s. The difference in the fluctuation state in numerically simulated and experimentally obtained results is attributed to material properties used for adhesive between the module and PCB substrate. Apart from the time of achieving the fluctuation state, the simulated temperature curves are in a good agreement with experimental results. The results can be used for a parametric study, and to corroborate the temperature analysis. The temperature feedback control system is also tested for transient ambient temperature conditions. Fig. 10 shows the time variation of temperature of the deformable mirror module as the ambient temperature changes from 0 °C to 40 °C. The temperature of the module is well controlled at the operating temperature, and the obtained magnitude of the temperature fluctuation is about ±0.5 °C. Thus it could be concluded that the developed temperature feedback control system shows good performance with the variation of ambient temperature. Fig. 11 shows the image test for the micro beam projector. The black and white colors represent the maximum movements of deformable mirrors. The

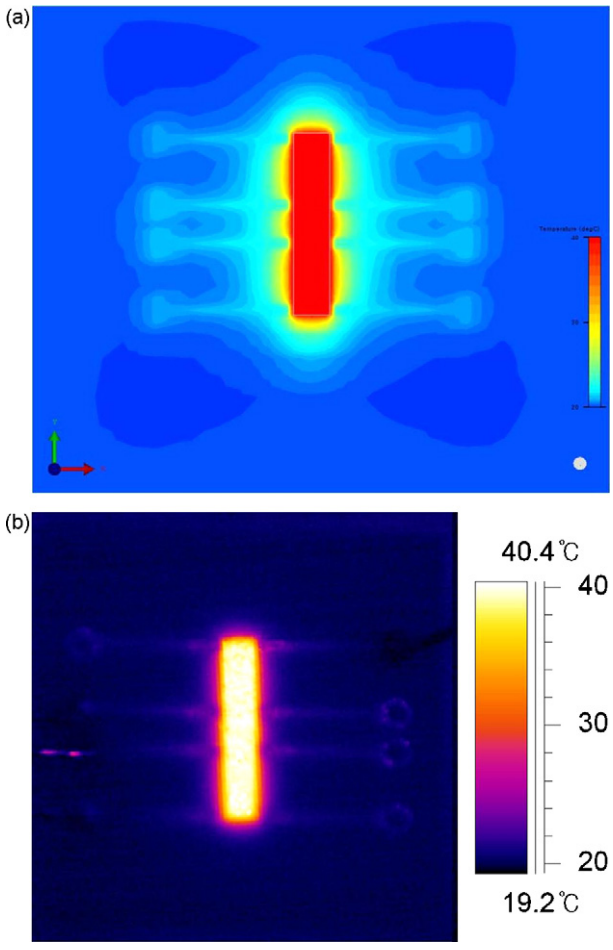

Fig. 8. (a) Temperature distribution of deformable mirror module. (b) Temperature distribution of deformable mirror module.

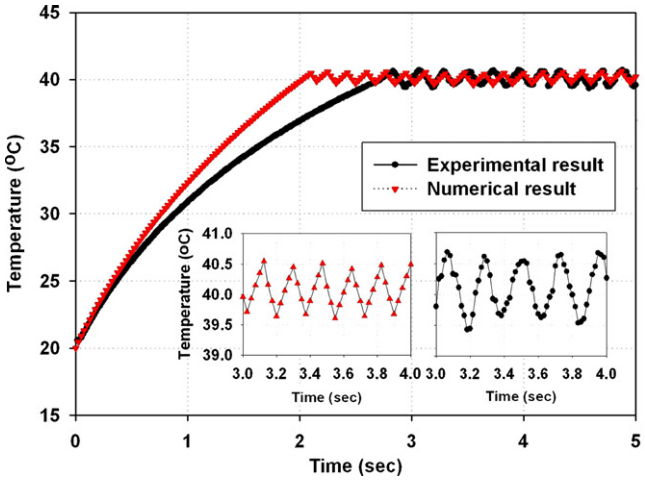

Fig. 9. Time variation of temperature of the deformable mirror module.

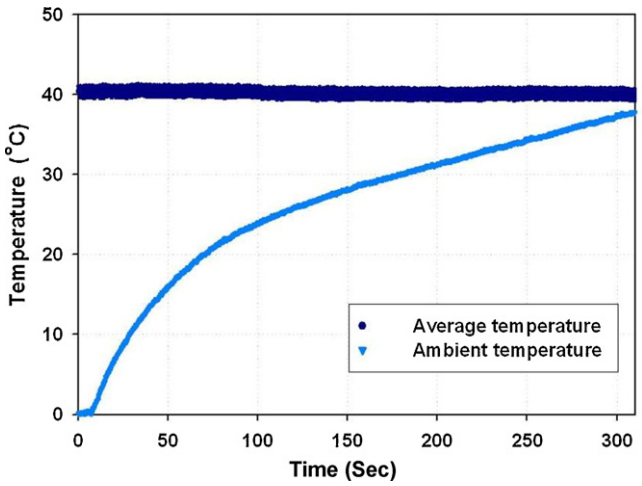

Fig. 10. Temperature of the deformable mirror module in variant ambient temperature.

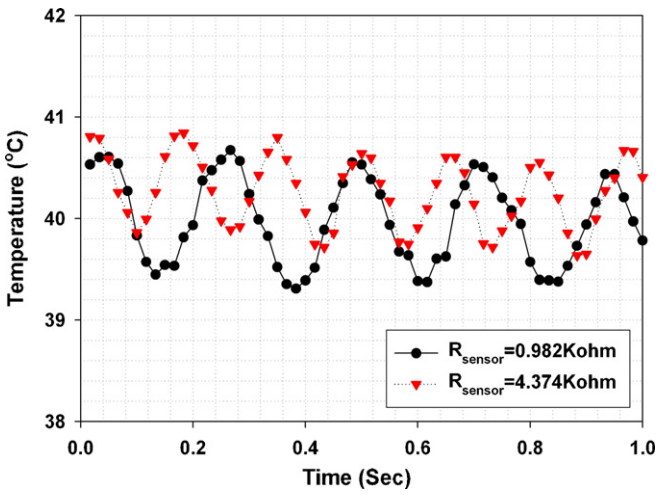

Fig. 12. Temperature fluctuations of the deformable mirror module.

original image of PADP is shown in Fig. 11(a). Fig. 11(b) and (c) shows the images when the difference between the actual temperature and the optimal temperature, ΔT, is 16 °C and 23 °C respectively. It could be seen that the image quality decreases as temperature difference increases. The image, however, returns to its original state when the developed control system is used (see Fig. 11(d)).

4.4. Device performance

The MOSFET, comparator, and Pt temperature sensors, shown in Fig. 4, are the important components in the performance of the temperature feedback control system. From the results shown in Fig. 9, the most important component is the Pt temperature sensor, because its switching period is longer than the operating time of the MOSFET and comparator. In order to improve device performance, four resistance values are used. Fig. 12 shows the module temperature fluctuations versus operating time. The magnitude of temperature fluctuations and the time period for which the microheater is are shown in Fig. 13. The frequency of switching on the microheater is increased with the magnitude of R_{sensor}. The reduction in time period during which the microheater is on reduces the magnitude of temperature fluctuations. Therefore, the increase in the resistance of the Pt temperature sensor can reduce the length of time the microheater is switched on. This results in more precise temperature management.

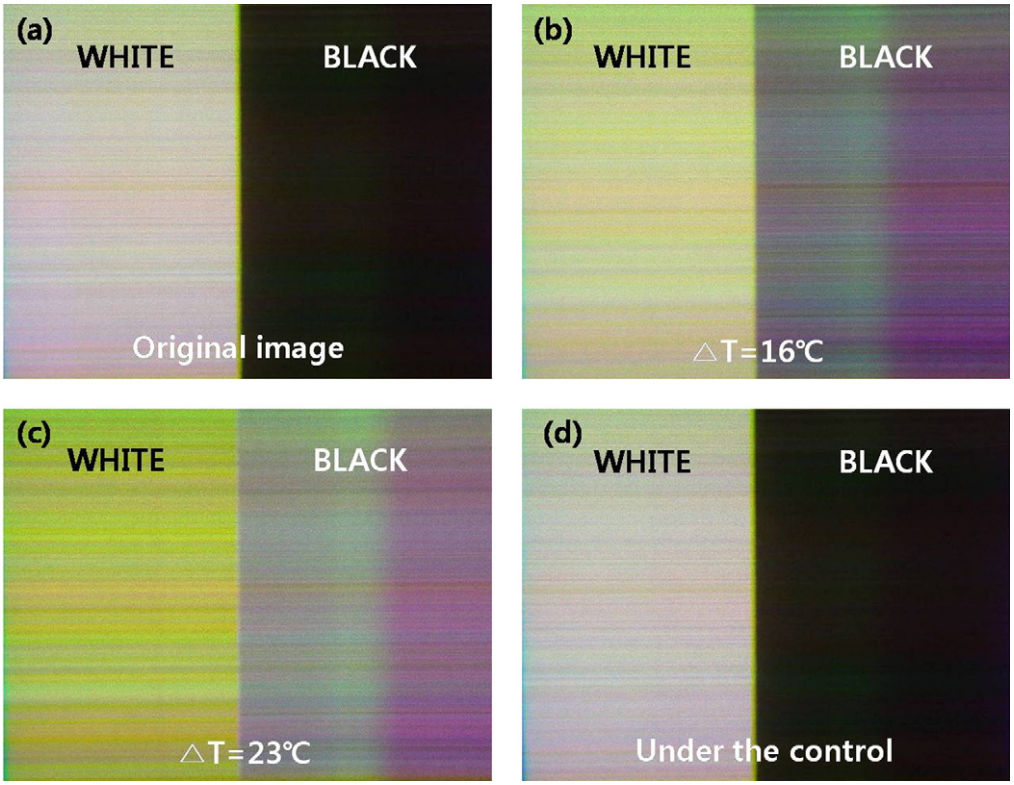

Fig. 11. Image test using developed system.

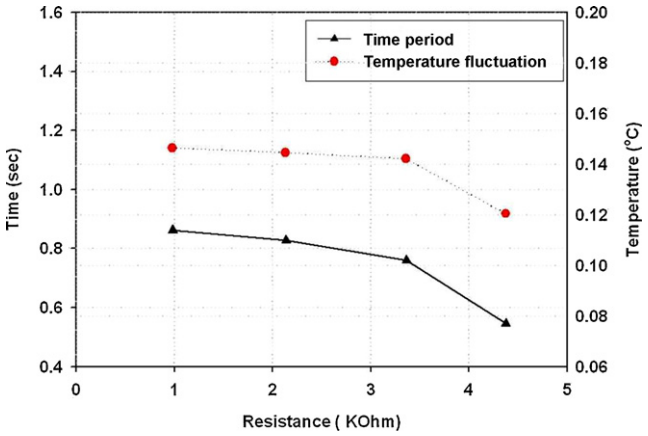

Fig. 13. Operation time and magnitude of temperature fluctuation.

5. Conclusion

This paper describes the design, fabrication, simulation, and testing of a temperature feedback control system using a microheater on a PADP. The temperature feedback control system is concluded to be a potential solution for the thermal problems associated with the display package. Using this system, module temperature can be continuously controlled with a ±0.5 °C fluctuation in the 0–40 °C temperature range. In the operating regime this temperature is maintained at 40 °C. The operation of the microheater and its feedback control are modeled using the switching period. The operating effects of the microheater are investigated computationally and compared against the experimental results. The magnitude of the temperature fluctuations, and the switching period, are studied for four resistances of different magnitudes. It is observed that the performance of the temperature feedback control improves with the increase in the resistance of the Pt temperature. Consequently, the proposed temperature control system can be used to improve display package performance, and can be useful in the implementation of piezoelectric actuators into commercial electronic devices.

Acknowledgment

This work was supported by IITA in Korea MIC, Leading Edge R&D Program.

References

[1] S.K. Yun, et al., A novel diffractive micro-optical modulator for mobile display applications, in: SPIE Proceeding 6887, 2008, pp. 688702–688711.
[2] K. Kano, et al., Temperature dependence of piezoelectric properties of sputtered AlN on silicon substrate, Sensors and Actuators A 130–131 (2006) 297–402.
[3] T. Li, et al., Frequency dependence of piezoelectric vibration velocity, Sensors and Actuatrors A 138 (2007) 404–410.
[4] D. Bouyge, et al., Integration of micro-electro-mechanical deformable mirrors in doped fiber amplifiers, in: Symposium o Design, Test, Integration and Packaging of MEMS/MOEMS, Stresa – Italy, 26–28 April 2006, 2007, pp. 1607–1613.
[5] Isolde Simon, et al., Micromachined metal oxide gas sensors: opportunities to improve sensor performance, Sensors and Actuators B 73 (2001) 1–26.
[6] M. Graf, et al., Transistor heater for microhotplate-based metal-oxide microsensors, Electron Device Letters, IEEE 26 (2005) 295–297.
[7] J.-W. Gong, et al., Temperature feedback control for improving the stability of a semiconductor-metal-oxide (SMO) gas sensor, IEEE Sensors Journal 6 (1) (2006) 139–145.
[8] G.-S. Chung, Fabrication and characterization of micro-heaters with low-power consumption using SOI membrane and trench structures, Sensors and Actuators A 112 (2004) 55–60.
[9] R.C. Jaeger, Introduction to Microelectronic Fabrication, 2nd ed., Prentice-Hall, Upper Saddle River, NJ, 2002.
[10] R.C. Weast, et al., Handbook of Chemistry and Physics, 66th ed., CRC, Boca Raton, FL, 1985–1986, pp. F-120–F-120.
[11] M.G. Pecht, et al., Electronic Packaging Materials and their Properties, CRC Press, Boca Raton, 1998.
[12] National Semiconductor Corporation, LM339 M datasheet, 2004.
[13] International Rectifier, IRL530N datasheet, 2004.
[14] S.P. Overmann, Thermal design considerations for portable DLP™ projectors, in: The 34th International Symposium on Microelectronics, 2001.